

Chapter 7

Results

7.1 Blind results

The blind results after all corrections, including set-dependent uncertainties, are shown in Table 7.1. The uncorrected results, the corrections and the set-dependent uncertainties are listed separately in Tables 7.2 and 7.3. The results are determined independently for each of the energy calibration approaches (shift and scale) that were described in Section 6.7.2. The results for the energy calibration applied as a shift are shown in Fig. 7.1, where there is good consistency over the chosen sets. Sets 72 (TECs-in), 76 (muon beam steered in θ_y) and 86 (muon beam steered in x and θ_x) were used to evaluate the systematic uncertainty for the polarisation; they have significantly larger polarisation uncertainties that have not been evaluated, and are therefore not included in the final result. Sets 70 and 71 were taken at different central magnetic field strengths; they are excluded from the final $P_\mu^\pi \xi$ result since the fringe field validation was only carried out at a central field strength of 2.0 T. The weighted average of $\Delta P_\mu^\pi \xi$ is 79.8×10^{-4} when the energy calibration is applied as a shift, and 80.7×10^{-4} for a scale. Averaging over these results, and including an additional statistical uncertainty from determining the relaxation rate (see Section 6.2.10), the final blind result is

$$\Delta P_\mu^\pi \xi = [80.3 \pm 3.5 \text{ (stat.)}_{-6.3}^{+16.5} \text{ (syst.)}] \times 10^{-4}. \quad (7.1)$$

The fit quality for each set is shown in the table of uncorrected results (Table 7.2). For a nominal set, the normalised residuals are shown explicitly in Fig. 7.2. The fit quality is excellent for all sets, and there is no evidence that the normalised residuals depend on momentum or angle.

Table 7.1: Blind results, *after* all corrections, including set-dependent uncertainties.

Set	Target	Description	Shift energy calib.	Scale energy calib.
			$\Delta P_{\mu}^{\xi} (\times 10^{-4})$	$\Delta P_{\mu}^{\xi} (\times 10^{-4})$
68	Ag	Stopping distrib. peaked $\frac{1}{3}$ into target	90.2 ± 7.6	90.3 ± 7.6
74	Ag	Nominal A	83.7 ± 7.5	83.9 ± 7.5
75	Ag	Nominal B	85.5 ± 6.4	85.9 ± 6.4
83	Al	Downstream beam package in place	80.7 ± 6.6	82.2 ± 6.6
84	Al	Nominal C	69.1 ± 6.9	70.8 ± 6.9
87	Al	Nominal D	82.5 ± 6.7	83.6 ± 6.7
91	Al	Lower momentum I	82.2 ± 13.0	83.0 ± 13.0
92	Al	Lower momentum II	73.5 ± 11.2	75.0 ± 11.2
93	Al	Lower momentum III	62.1 ± 9.2	63.8 ± 9.2
70	Ag	B = 1.96 T	79.0 ± 6.3	80.0 ± 6.3
71	Ag	B = 2.04 T	93.2 ± 6.6	93.3 ± 6.6
72	Ag	TECs-in, nominal beam	90.7 ± 6.4	91.1 ± 6.4
76	Ag	Steered beam A	33.2 ± 7.0	33.6 ± 7.0
86	Al	Steered beam B	52.7 ± 6.2	54.6 ± 6.2

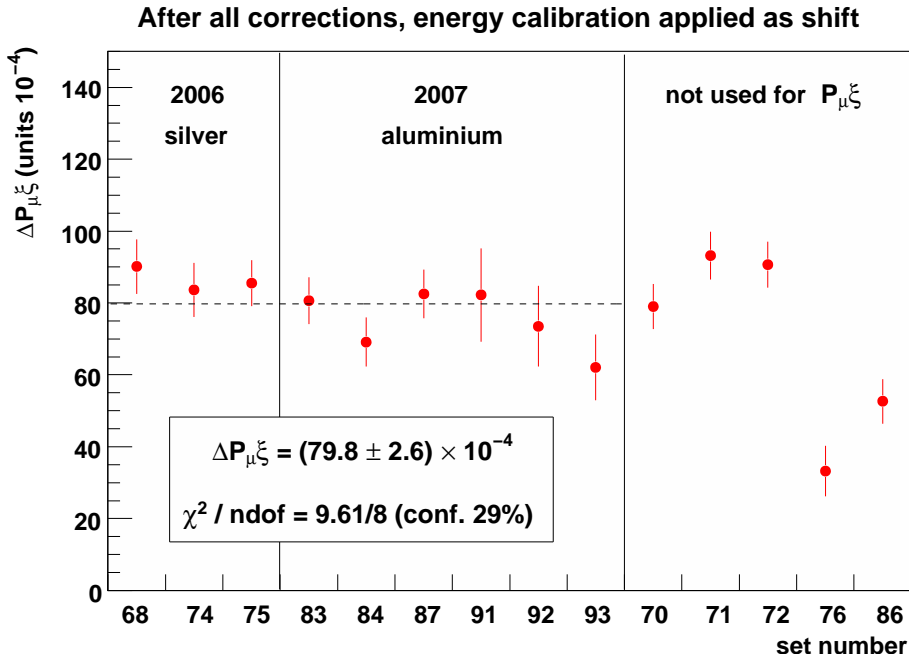

 Figure 7.1: Consistency of $\Delta P_{\mu}^{\pi\xi}$, the difference in $P_{\mu}^{\pi\xi}$ between the data and a hidden value in the simulation.

Table 7.2: Blind results, *before* any corrections.

Set	Energy calibration applied as a shift			Energy calibration applied as a scale		
	χ^2/ndf	Confidence	$\Delta P_\mu \xi (\times 10^{-4})$	χ^2/ndf	Confidence	$\Delta P_\mu \xi (\times 10^{-4})$
68	2384/2439	78.3	84.9 ± 7.6	2373/2439	82.7	84.9 ± 7.6
74	2440/2439	49.3	78.3 ± 7.5	2450/2439	43.7	78.5 ± 7.5
75	2453/2439	41.8	80.6 ± 6.4	2452/2439	42.2	80.8 ± 6.4
83	2405/2439	68.5	75.3 ± 6.5	2416/2439	62.5	76.8 ± 6.5
84	2515/2439	13.8	63.6 ± 6.8	2510/2439	15.4	65.2 ± 6.8
87	2411/2439	65.5	77.1 ± 6.7	2407/2439	67.6	78.1 ± 6.7
91	2564/2439	3.9	71.4 ± 12.9	2578/2439	2.5	72.0 ± 12.9
92	2474/2439	30.7	63.3 ± 11.1	2479/2439	28.2	64.7 ± 11.1
93	2504/2439	17.4	52.5 ± 9.0	2518/2439	13.1	54.1 ± 9.0
70	2370/2439	84.0	74.0 ± 6.3	2380/2439	80.0	74.9 ± 6.3
71	2425/2439	57.6	88.1 ± 6.6	2430/2439	54.9	88.1 ± 6.6
72	2513/2439	14.4	85.8 ± 6.4	2508/2439	16.3	86.2 ± 6.4
76	2430/2439	55.2	27.5 ± 7.0	2423/2439	58.9	27.8 ± 7.0
86	2425/2439	57.7	47.7 ± 6.2	2424/2439	58.0	49.6 ± 6.2

Table 7.3: Set-dependent corrections and uncertainties for $\Delta P_\mu^\pi \xi$. These are described in Section 6.1.

Set	Corrections (units 10^{-4})				Set-dependent uncertainties (units 10^{-4})		
	Production target	Relaxation rate	Spectrum fitter	Energy calib. Scale	Energy calib. Shift	Energy calib. statistical	Production target
68	+0.9	+2.7	-0.5	+2.2	+2.3	± 0.5	± 0.3
74	+0.9	+2.7	-0.5	+2.3	+2.4	± 0.5	± 0.3
75	+0.9	+2.7	-0.5	+1.9	+2.0	± 0.4	± 0.3
83	+0.9	+3.3	-0.5	+1.7	+1.8	± 0.4	± 0.3
84	+0.9	+3.3	-0.5	+1.8	+1.9	± 0.4	± 0.3
87	+0.9	+3.3	-0.5	+1.8	+1.9	± 0.4	± 0.3
91	+5.9	+3.3	-0.5	+2.1	+2.2	± 0.9	± 1.9
92	+5.2	+3.3	-0.5	+2.2	+2.4	± 0.7	± 1.6
93	+5.2	+3.3	-0.5	+1.7	+1.7	± 0.6	± 1.6
70	+0.9	+2.7	-0.5	+1.9	+2.0	± 0.4	± 0.3
71	+0.9	+2.7	-0.5	+2.0	+2.1	± 0.4	± 0.3
72	+0.9	+2.7	-0.5	+1.8	+1.9	± 0.4	± 0.3
76	+0.9	+3.3	-0.5	+2.1	+2.2	± 0.4	± 0.3
86	+0.9	+3.3	-0.5	+1.3	+1.4	± 0.4	± 0.3

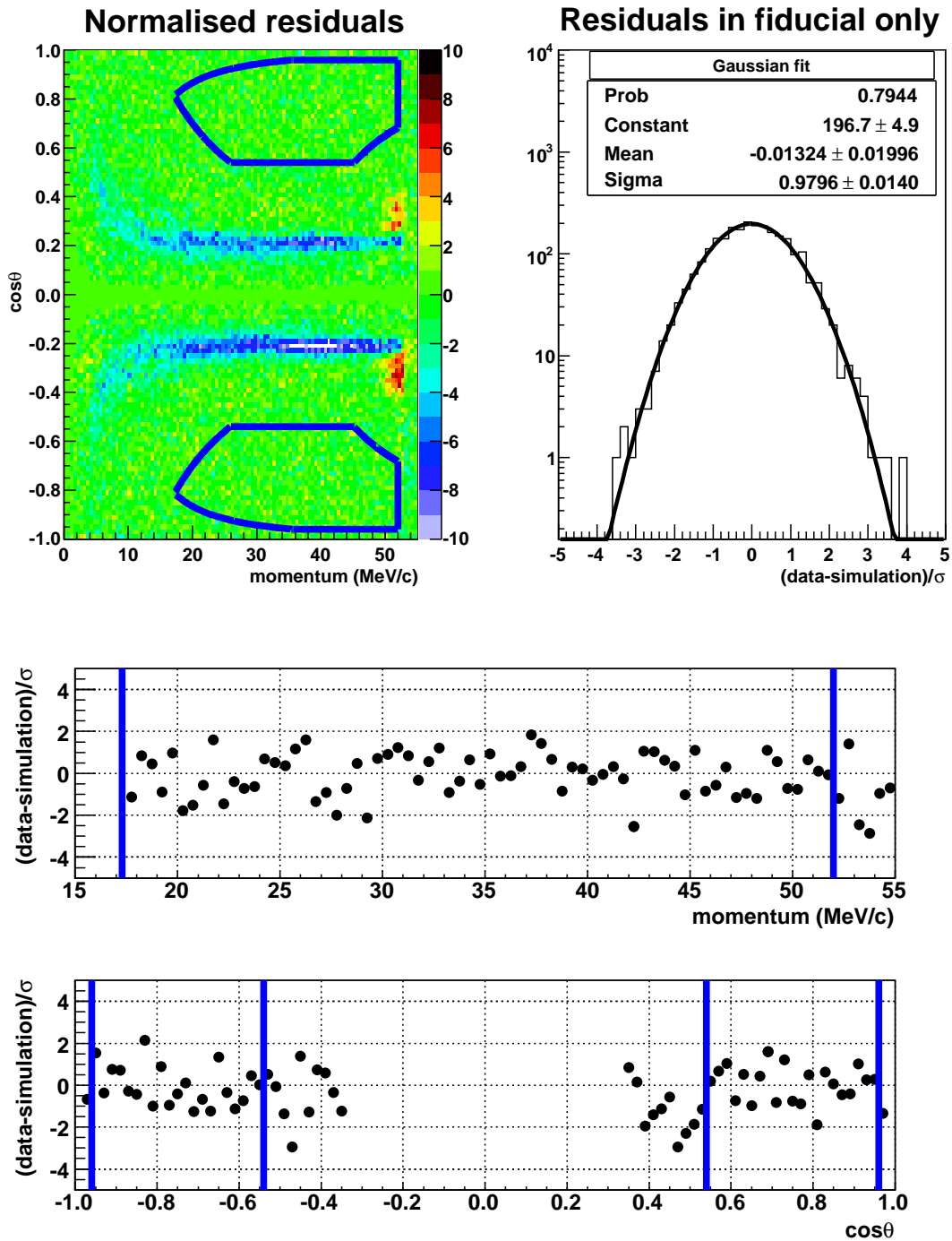


Figure 7.2: Normalised residuals from a spectrum fit of nominal data (set 87) to its accompanying simulation. The thick blue lines indicate the kinematic fiducial boundaries. Within the fiducial region there is no evidence of structure.

7.2 Result revealed

On 29 January 2010, the hidden value of ξ was revealed as

$$\xi_{\text{hidden}} = 0.99281. \quad (7.2)$$

This is added to the blind result in Eq. (7.1) to give

$$P_{\mu}^{\pi} \xi = 1.00084 \pm 0.00035 \text{ (stat.)}_{-0.00063}^{+0.00165} \text{ (syst.)}, \quad (7.3)$$

which agrees with all previous results for $P_{\mu}^{\pi} \xi$ and $P_{\mu}^K \xi$, and is consistent with the standard model values of $P_{\mu}^{\pi} = \xi = 1$. The new result is a factor of 3.2 more precise than the previous TWIST measurement, $P_{\mu}^{\pi} \xi = 1.0003 \pm 0.0006 \text{ (stat.)} \pm 0.0038 \text{ (syst.)}$ [21], and a factor of 7.0 more precise⁴⁴ than the pre-TWIST direct measurement, $P_{\mu}^{\pi} \xi = 1.0027 \pm 0.0079 \text{ (stat.)} \pm 0.0030 \text{ (syst.)}$ [67]. The new result is also compatible with a recent *indirect* measurement that used TWIST ρ and δ results, $0.99524 < P_{\mu} \xi \leq \xi < 1.00091$ (90% C.L.)[10]. Note that Eq. (7.3) is the final result of the TWIST $P_{\mu}^{\pi} \xi$ blind analysis, and this number will be published.

7.3 “White box” consistency test

A simulation is generated using the final result in Eq. (7.3) for ξ . The resulting spectrum is fit against the data. After applying all corrections, the result must come out consistent with zero for the consistency test to be passed. This is carried out twice (once for the silver target, and once for aluminium), and the results are

$$\Delta P_{\mu}^{\pi} \xi (\text{Al}) = (7.2 \pm 6.9) \times 10^{-4}, \quad (7.4)$$

$$\Delta P_{\mu}^{\pi} \xi (\text{Ag}) = (0 \pm ?) \times 10^{-4}. \quad (7.5)$$

These are consistent with zero, which confirms that all corrections have been applied properly.

⁴⁴In units of 10^{-4} , the uncertainty corresponding to \pm one standard deviation for the pre-TWIST direct measurement is $2 \times \sqrt{79^2 + 30^2} = 169$. For the current measurement, the positive error bar is $\sqrt{3.5^2 + 16.5^2} = 16.9$, and the negative error bar is $\sqrt{3.5^2 + 6.3^2} = 7.2$, giving the size of \pm one standard deviation as $16.9 + 7.2 = 24.1$. The improvement factor is then $169/24.1 = 7.0$.

7.4 Physics implications

The $P_\mu^\pi \xi$ result will be used in a global analysis, as described in Section 1.4.2. At the time of writing this analysis is not available in a final form, and will therefore not be discussed here.

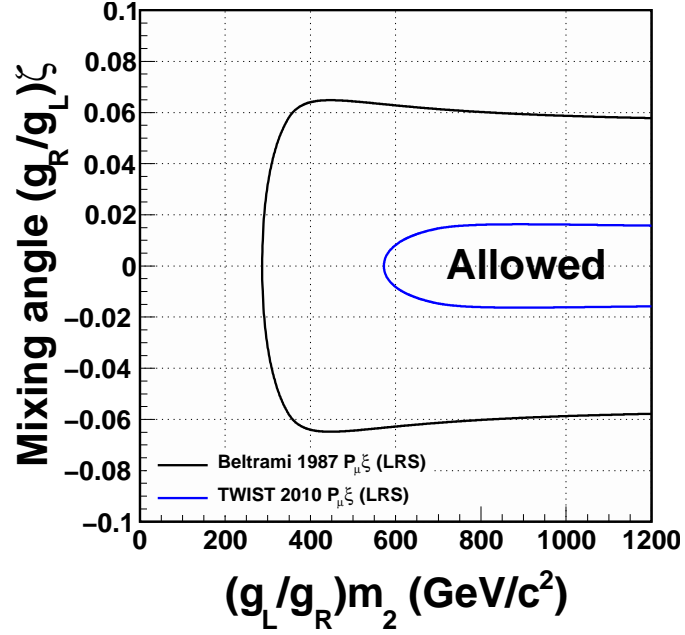
Several left-right symmetric (LRS) models were described in Section 1.5.2. The most restrictive is the manifest LRS model, where the weak coupling constants and CKM matrices are the same for left- and right-handed particles, and there is no CP violating phase. The generalised LRS model relaxes all of these requirements. An exclusion region for the manifest and generalised LRS models can be constructed at the 90% confidence level. After enforcing the requirement in the LRS models that $P_\mu^\pi \xi \leq 1$, the lower limit at 90% confidence is $[P_\mu^\pi \xi]_{90} = 0.99922$. This value is used in Eqs. (1.27)-(1.32) to produce Fig. 7.3, which compares the pre-TWIST direct $P_\mu^\pi \xi$ result with the value from the current analysis. In the generalised LRS model, the lower limit for an additional W-boson mass is increased from $(g_L/g_R)m_2 = 287 \text{ GeV}/c^2$ to $573 \text{ GeV}/c^2$, and in the manifest LRS, the lower limit is increased from $m_2 = 318 \text{ GeV}/c^2$ to $573 \text{ GeV}/c^2$. Note that Fig. 7.3 should not be used as the final TWIST exclusion region; a future publication will include the effect of the new TWIST ρ measurement, and will likely result in a more restrictive plot.

7.5 Future experiments

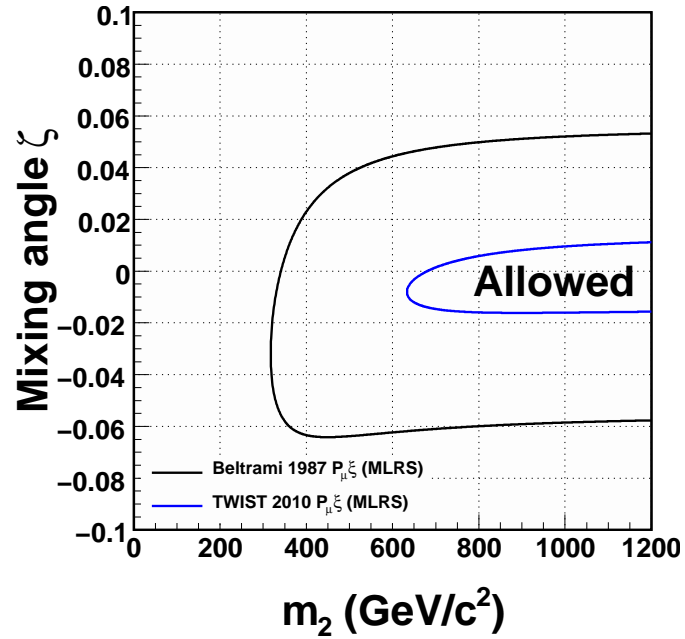
A $P_\mu^\pi \xi$ measurement with precision greater than 1×10^{-4} is possible with a TWIST-style experiment (*i.e.* longitudinally polarised muons delivered into the centre of uniform magnetic field, with high precision positron tracking). The uncertainties that limited the current measurement will be briefly discussed, with a view to how they could be reduced.

7.5.1 Statistical uncertainty

The statistical uncertainty for this measurement is already at the level of 3.5×10^{-4} , or just 2.5×10^{-4} for the part that originates from the decay spectrum fit. This was achieved with about four months of continuous data acquisition at a surface muon rate of $2000 - 5000 \text{ s}^{-1}$ (a significant amount of tuning over the years 2000 to 2006 was necessary to achieve the required beam quality). The statistical uncertainty of a future measurement could be reduced to commensurate levels by using a channel with an order of magnitude



(a) Generalised LRS model.



(b) Manifest LRS model.

Figure 7.3: Exclusion region (90% confidence limit) for ζ , the mixing angle between the left- and right-handed W -boson eigenstates, and $(g_L/g_R)m_2$, where g_L and g_R are the weak coupling constants for the predominantly left and right-handed W -bosons, and m_2 is the mass of the predominantly right-handed W -boson. The “Beltrami” entry refers to the pre-TWIST direct $P_\mu^\pi \xi$ measurement[67].

higher flux. For example, a new μ E4 channel at PSI already achieves this by placing radiation-hard solenoids close to the muon production target, allowing an acceptance of $\Delta\Omega \sim 135$ msr[81] compared to 29 msr from the M13 beam line. A higher rate would require an improvement in the data acquisition electronics, in order to prevent significant pileup. If the TWIST analysis approach were adopted, using an accompanying simulation to include inefficiencies and biases, then the simulation statistics could be significantly increased by taking advantage of faster CPUs.

7.5.2 Magnetic field map uncertainty

The dominant systematic uncertainty from the fringe field could be reduced. We used an MRI magnet surrounded by a custom steel yoke, but a specially constructed magnet could provide a more gradual fringe field by increasing the z -distance over which the field reaches its full strength. Alternatively, or additionally, a higher-rate muon channel would allow the possibility of beam collimation; by selecting low angle muons that undergo very little depolarisation, the uncertainty on that depolarisation would be decreased. However, such collimators could introduce an additional uncertainty from muons scattering off them, and this would have to be carefully assessed; active collimation may help to reduce problems.

The measurement of our magnetic field could have been done better. A future experiment would need alignments of the measuring apparatus under control at the < 0.5 mm and < 1 mrad level, and should measure all three components of the magnetic field. If the three components are measured with more than one probe, then the relative orientation of the probes must be known with high precision, and a correction may be necessary for the probes not being at exactly the same point in space; a smaller field gradient would also help here. Also, the current experiment would have benefited from field measurements at finer space intervals (in all coordinates) over the region that the muons actually traversed.

We used the `Opera` magnetic field simulation to produce the B_x and B_y components of our field map. With all three components measured, it may not be necessary to have a magnetic field simulation at all, although an alternative method of smoothing the field measurements would be necessary. If a simulation is required, it is recommended that more than one piece of software be used; for example, the latest version of `Opera`[85], or the COMSOL Multiphysics (formerly FEMLAB) software[105].

The TWIST approach was to measure the muons before the fringe field, and rely on a `GEANT3` simulation to predict the final polarisation. There are at least two ways to improve the confidence in the final polarisation: first the spin could be transported by

one or more independent simulations; second the beam could be steered off-axis in order to lower the polarisation, and a simulation’s ability to reproduce the polarisation change from the data would allow confidence to be gained. As seen in this thesis, the alignment of the beam and the field must be under strict control in order for the second approach to work.

The time expansion chambers (TECs) that measured our muon beam had adequate precision, but suffered from alignment uncertainties and aging problems that would be more significant for a future measurement. An improved measurement using a similar device would have to address these issues. A significant uncertainty from the TECs originated from the simulation’s ability to correct for the multiple scattering that takes place while the muons pass through the active volume; a subsidiary experiment may be needed to validate the simulation’s accuracy in making this correction.

An alternative proposal put forward by a TWIST collaborator is to measure the muon beam inside the strong magnetic field[106, 107]. This would present a greater engineering and analysis challenge, since the device would have to work in a strong magnetic field and the reconstructed trajectories would be helices. If carried out accurately, this approach has the potential to eliminate many of the problems associated with simulating the spin.

7.5.3 Stopping material depolarisation uncertainty

For the current measurement the polarisation’s relaxation rate was measured using the normal data. A subsidiary μ^+ SR experiment provided a consistent but uncompetitive result. A future experiment should consider an integrated “ μ^+ SR mode”, with a higher beam intensity and a simple analysis that only identifies particles and their times. The goal should be to unequivocally determine the form of $P_\mu(t)$ and its parameters. Since this experimental mode would not measure the absolute polarisation, a Wien filter should be considered to significantly reduce the beam positrons, which would allow a much higher muon rate. (A μ^+ SR analysis was considered using the existing TWIST detector. The proportional chambers (PCs) had a timing resolution of ~ 20 ns, and could identify particles based on their pulse width. This would have allowed us to use decay data below $1 \mu\text{s}$ to better determine the relaxation rate. However, the suggestion came at a late stage in the analysis and would have required significant software changes to implement.)

If a “ μ^+ SR mode” is not possible, then a subsidiary μ^+ SR experiment should be considered from the outset. Suggestions are made in Section H.9 that would allow a better time differential μ^+ SR measurement. Another useful measurement could be provided by

a pulsed muon setup such as that of the Rutherford Appleton Laboratory (UK).

For the TWIST polarisation measurements, only aluminium and silver targets were used. Additional targets that produced consistent $P_\mu^\pi \xi$ measurements would strengthen a future result.

We were able to successfully eliminate muons that stopped in the gas before our stopping target; a stricter cut could have further reduced the contamination, with a loss of statistical precision. However, one surprise was our simulation’s prediction that 0.11% of muons passed through the metal stopping target and entered PC7, but did not have enough energy to produce a signal. A more careful simulation of the PC response would have allowed us to determine this fraction better, and correct $P_\mu^\pi \xi$ accordingly.

7.5.4 Other uncertainties

The uncertainty from production target scattering can be reduced in three ways: i) by selecting a smaller momentum resolution, which would be feasible with a higher intensity beam line, ii) by a more accurate validation of the multiple scattering within the simulation, iii) if one could select a wide range of sub-surface muon momenta, then muons from much deeper within the production target could be selected; the difference in polarisation between the lower momentum muons and the surface muons would then help to validate the simulation of multiple scattering.

There are theoretical considerations at the $< 1 \times 10^{-4}$ level that would be important for future measurements. The next level of radiative corrections (full $O(\alpha^3)$) would ideally be evaluated. A calculation of radiative corrections that does not assume an underlying ($V - A$) interaction would be very welcome, although this would need a suitable renormalisable theory. The pion radiative decay mode should also be considered more carefully; such calculations have been carried out for the purposes of TWIST[108].

The track reconstruction efficiency and resolution were both measured here using a special analysis with the muons stopped at the entrance of the spectrometer, and the decay positron reconstructed separately in each half of the detector. A future experiment should consider designing the beam line to allow a “spread muon tune”, where the muons stop close to the detector entrance but are spread out over a much wider area than usual. In addition, the stopping target should be as large as possible to allow a wide range of decay positron phase space to be reconstructed in each detector half. Also the ability to rotate the entire detector (*i.e.* swap the upstream and downstream ends) would provide a more stringent test of measurements that compare the upstream and downstream response

of the detector.

The uncertainties from positron interactions (mostly δ -electrons and bremsstrahlung) will need careful consideration. This may require work by theorists, or a comparison of several simulations that claim to accurately reproduce these processes in the relevant energy range. A future experimenter should consider a subsidiary experiment to help understand these processes better in the low energy range.

Another area requiring thought is the energy calibration. Inevitably a correction or calibration will be needed since the decay positron reconstruction will have subtle biases and systematic errors. The method of measuring and then propagating such a correction will likely be dominant in a future $P_\mu^\pi \xi$ measurement. For the TWIST experiment this correction was due to a complex combination of errors in the magnetic field map, imperfect drift cell space-time-relationships, bias from the helix fitting, the energy-loss model in the simulation, multiple scattering of the decay positron and uncertainties in the stopping distribution; these pieces could not be disentangled, and, as a result, a conservative approach was taken in the propagation of the energy calibration to the bulk of the decay spectrum. A future experiment must consider ways of eliminating these errors, or breaking them into orthogonal pieces; see Ref. [97] for more information.

The remaining uncertainties from Table 6.1 could have easily been reduced. The beam intensity uncertainty could be eliminated by tuning the simulation's muon rate to properly match the data, using the R_μ criteria described in Section 6.8.1. The uncertainty from background muons could be reduced by tuning the stopping distribution based on the α_{diff} criteria in Section 6.2.12, and/or adding to the simulation a source of pions at the end of the M13 beam line. The refined space-time-relationships in the DCs and the wire time offsets were already adequate for a measurement at the $< 1 \times 10^{-4}$ level. The strict engineering requirements of the TWIST detector meant that alignment uncertainties were already at a negligible level. The outside material systematic could be eliminated by adding more detail to the geometry of the simulation outside of the active detector region. The η correlation will be reduced for future measurements after a global analysis using this $P_\mu^\pi \xi$ measurement and the simultaneous ρ and δ measurements.

In addition to the goal of extracting $P_\mu^\pi \xi$ (and ρ , δ), a future experiment should consider subsidiary measurements that may even benefit the main experiment. An η measurement from the decay spectrum would provide a validation of the results that use the transverse polarisation of the decay positron, although positron interactions would have to be thoroughly understood since η affects the low momentum end of the spectrum. Some extensions to the standard model postulate additional parameters to describe the

decay spectrum; see Ref. [79] for a more detailed discussion. The *negative* muon decay spectrum for each stopping target could be produced using the same analysis software; see Ref. [109] for such a measurement (the first of its kind) that used the TWIST apparatus. Lastly, if there was a possibility to switch between muons sourced from pions and kaons, then the resulting $P_\mu^\pi \xi$ and $P_\mu^K \xi$ measurements would provide a more complete test of the standard model.

7.6 Conclusions

The quantity $\Delta P_\mu^\pi \xi$, the difference between $P_\mu^\pi \xi$ and a hidden simulation value, has been measured as

$$\Delta P_\mu^\pi \xi = [80.3 \pm 3.5 \text{ (stat.)}_{-6.3}^{+16.5} \text{ (syst.)}] \times 10^{-4}. \quad (7.6)$$

This is the final direct $P_\mu^\pi \xi$ measurement from the TWIST collaboration, and is a factor of 7.0 more precise than the pre-TWIST result[67]. The result improves the limits on the mass of an additional right-handed W-boson in left-right symmetric models, and will be used to limit extensions to the standard model in a global analysis of muon decay data.

Bibliography

- [1] S. Weinberg. A Model of Leptons. *Phys. Rev. Lett.*, 19(21):1264–1266, Nov 1967.
- [2] Donald Hill Perkins. *Introduction to High-Energy Physics; 4th ed.* Cambridge Univ. Press, Cambridge, 2000.
- [3] C. Amsler *et al.* Review of Particle Physics. *Phys. Lett. B*, 667(1-5):1–6, 2008. Review of Particle Physics.
- [4] D. Griffiths. *Introduction to Elementary Particles.* Wiley, 1987.
- [5] M. Goldhaber, L. Grodzins, and A. W. Sunyar. Helicity of Neutrinos. *Phys. Rev.*, 109:1015 – 1017, 1958.
- [6] D. Binosi and L. Theußl (sic.). JaxoDraw: A graphical user interface for drawing Feynman diagrams. *Comput. Phys. Commun.*, 161:76–86, August 2004.
- [7] C.A. Gagliardi, R.E. Tribble and N.J. Williams. Global analysis of muon decay measurements. *Phys. Rev. D*, 72(7):073002, Oct 2005.
- [8] W. Fetscher, H.-J. Gerber and K.F. Johnson. Muon decay: complete determination of the interaction and comparison with the standard model. *Phys. Lett. B*, 173(1):102–106, 1986.
- [9] S. Eidelman *et al.* Review of Particle Physics. *Phys. Lett. B*, 592(1-4):1–5, 2004. Review of Particle Physics.
- [10] R.P. MacDonald *et al.* Precision measurement of the muon decay parameters ρ and δ . *Phys. Rev. D*, 78(3):032010, 2008.
- [11] A. Sirlin, New York University, USA. Private communication.
- [12] A. B. Arbuzov. First-order radiative corrections to polarized muon decay spectrum. *Phys. Lett. B*, 524(1-2):99 – 106, 2002.

- [13] A. Arbuzov, A. Czarnecki and A. Gaponenko. Muon decay spectrum: Leading logarithmic approximation. *Phys. Rev. D*, 65:113006, 2002.
- [14] A. Arbuzov and K. Melnikov. $\mathcal{O}(\alpha^2 \ln(m_\mu/m_e))$ corrections to electron energy spectrum in muon decay. *Phys. Rev. D*, 66:093003, 2002.
- [15] A. Arbuzov. Higher order QED corrections to muon decay spectrum. *J. High Energy Phys.*, 2003(03):063–063, 2003.
- [16] K. Melnikov C. Anastasiou and F. Petriello. The electron energy spectrum in muon decay through $\mathcal{O}(\alpha^2)$. *J. High Energy Phys.*, (09):014, 2007.
- [17] N. Danneberg *et al.* Muon Decay: Measurement of the Transverse Polarization of the Decay Positrons and its Implications for the Fermi Coupling Constant and Time Reversal Invariance. *Phys. Rev. Lett.*, 94:021802, 2005.
- [18] C. Gagliardi, Texas A&M University, Texas, USA. Private communication.
- [19] P. Herczeg. On muon decay in left-right-symmetric electroweak models. *Phys. Rev. D*, 34(11):3449–3456, Dec 1986.
- [20] V.M. Abazon *et al.* Search for W' Bosons Decaying to an Electron and a Neutrino with the D0 Detector. *Phys. Rev. Lett.*, 100:031804, 2008.
- [21] B. Jamieson *et al.* Measurement of $P_\mu \xi$ in polarized muon decay. *Phys. Rev. D*, 74(7):072007, 2006.
- [22] J.D. Jackson. *Classical Electrodynamics*. John Wiley & Sons, 1999.
- [23] V. Bargmann, L. Michel and V.L. Telegdi. Precession of the Polarization of Particles Moving in a Homogeneous Electromagnetic Field. *Phys. Rev. Lett.*, 2:435–436, 1959.
- [24] A. Balakin, V. Kurbanova and W. Zimdahl. Precession of a particle with anomalous magnetic moment in electromagnetic and gravitational pp-wave fields. *Gravity Cosmology Supplement*, 82:6–9, 2002.
- [25] P. Depommier. The BMT equation. Presentation to TWIST collaboration, May 2006.
- [26] P. Depommier. Muon depolarization in multiple scattering (TN100). Technical report, TWIST collaboration, TRIUMF, 2005.

-
- [27] W.H. Koppenol. Names for muonium and hydrogen atoms and their ions(IUPAC Recommendations 2001). *Pure Appl. Chem.*, 73:377–379, 2001.
- [28] M. Senba. Muon spin depolarization in noble gases during slowing down in a longitudinal magnetic field. *J. Phys. B: At. Mol. Opt. Phys.*, 31:5233–5260, 1998.
- [29] A. Jodidio *et al.* Search for right-handed currents in muon decay. *Phys. Rev. D*, 34(7), 1986.
- [30] A. Jodidio *et al.* Erratum: Search for right-handed currents in muon decay. *Phys. Rev. D*, 37(1), 1988.
- [31] J. H. Brewer. Muon spin rotation/relaxation/resonance. In *Encyclopedia of Applied Physics 11*, pages 23–53. 1994.
- [32] S.F.J. Cox. Implanted muon studies in condensed matter science. *J. Phys. C: Solid State Phys*, 20:3187–3319, 1987.
- [33] O. Hartmann *et al.* Diffusion of positive muons in some cubic metals. *Phys. Lett. A*, 61(2):141 – 142, 1977.
- [34] J. Brewer, University of British Columbia, Canada. Private communication.
- [35] W.B. Gauster *et al.* Measurement of the depolarization rate of positive muons in copper and aluminum. *Solid State Commun.*, 24(9):619–622, 1977.
- [36] W. Schilling. The physics of radiation damage in metals. *Hyperfine Interact.*, 4:636–644, 1978.
- [37] D.K. Brice. Lattice atom displacements produced near the end of implanted μ^+ tracks. *Phys. Lett. A*, 66:53–56, 1978.
- [38] P. Dalmas de Réotier and A. Yaouanc. Muon spin rotation and relaxation in magnetic materials. *J.Phys: Condens. Matter*, 9:9113–9166, 1997.
- [39] P. Dalmas de Réotier and A. Yaouanc. Quantum calculation of the muon depolarization function: effect of spin dynamics in nuclear dipole systems. *J.Phys: Condens. Matter*, 4:4533–4556, 1992.
- [40] A. Abragam. *Principles of Nuclear Magnetism*. International series of monographs on physics. Oxford University Press, 1986.

- [41] R.S. Hayano *et al.* Zero- and low-field spin relaxation studied by positive muons. *Phys. Rev. B*, 20:850, 1979.
- [42] W.J. Kossler *et al.* Diffusion and Trapping of Positive Muons in Al:Cu Alloys and in Deformed Al. *Phys. Rev. Lett.*, 41:1558–1561, 1978.
- [43] O. Hartmann *et al.* Coherent Propagation and Strain-Induced Localization of Muons in Al. *Phys. Rev. Lett.*, 41:1055–1058, 1978.
- [44] K.W. Kehr *et al.* Muon diffusion and trapping in aluminum and dilute aluminum alloys: Experiments and comparison with small-polaron theory. *Phys. Rev. B*, 26:567–589, 1982.
- [45] K.W. Kehr. Empirical information on quantum diffusion. *Hyperfine Interact.*, 17-19:63–74, 1984.
- [46] O. Hartmann. Diffusion and trapping of muons in aluminum: New experiments and comparison with Kondo theory. *Phys. Rev. B*, 37:4425–4440, 1988.
- [47] O. Hartmann. New results on diffusion in fcc metals. *Hyperfine Interact.*, 64:641–648, 1990.
- [48] O. Hartmann *et al.* Studies of μ^+ Localization in Cu, Al, and Al alloys in the Temperature Interval 0.03 – 100 K. *Phys. Rev. Lett.*, 44:337–340, 1980.
- [49] D.P. Stoker *et al.* Search for Right-Handed Currents by Means of Muon Spin Rotation. *Phys. Rev. Lett.*, 54:1887–1890, 1985.
- [50] D.P. Stoker, University of California, Irvine, USA. Private communication.
- [51] J. Korrynga. Nuclear magnetic relaxation and resonance (sic.) line shift in metals. *Physica*, 7-8:601–610, 1950.
- [52] S.J. Blundell and S.F.J. Cox. Longitudinal muon spin relaxation in metals and semimetals and the Korringa law. *J. Phys.: Condens. Matter*, 13:2163–2168, 2001.
- [53] J.H. Brewer *et al.* *Positive muons and muonium in matter*. Muon Physics. Academic Press Inc (London) Limited, 1975.
- [54] S.F.J. Cox *et al.* Muon Korringa relaxation. *Physica B*, 289-290:594–597, 2000.

-
- [55] R.H. Heffner. Muon spin depolarization in nonmagnetic metals doped with paramagnetic impurities. *Hyperfine Interact.*, 8:655–662, 1981.
- [56] J.A. Brown *et al.* Muon Depolarization by Paramagnetic Impurities in Nonmagnetic Metals. *Phys. Rev. Lett.*, 47:261–264, 1981.
- [57] B. Jamieson. *Measurement of the muon decay asymmetry parameter with the TWIST spectrometer*. PhD thesis, University of British Columbia, 2006.
- [58] T.D. Lee and C.N. Yang. Question of Parity Conservation in Weak Interactions. *Phys. Rev.*, 104(1):254–258, Oct 1956.
- [59] ARGUS collaboration. Determination of the Michel Parameters ρ , ξ , and δ in τ -Lepton Decays with $\tau \rightarrow \rho\nu$ Tags. *Phys. Lett. B*, 431:179–187, 1998.
- [60] L3 Collaboration. Measurement of the Michel parameters and the average tau-neutrino helicity from tau decays at LEP. *Phys. Lett. B*, 438:405–416, 1998.
- [61] R. Bartoldus. Measurements of the Michel Parameters in Leptonic Tau Decays using the OPAL Detector at LEP. *Nucl. Phys. B (Proc. Suppl.)*, 76:147–157, 1999.
- [62] R.L. Garwin, L.M. Lederman and M. Weinrich. Observations of the Failure of Conservation of Parity and Charge Conjugation in Meson Decays: the Magnetic Moment of the Free Muon. *Phys. Rev.*, 105:1415, January 1957.
- [63] G. R. Lynch, J. Orear, and S. Rosendorff. Muon decay in nuclear emulsion at 25 000 gauss. *Phys. Rev.*, 120(6):2277, Dec 1960.
- [64] M. Bardon, D. Berley, and L. M. Lederman. Asymmetry parameter in muon decay. *Phys. Rev. Lett.*, 2(2):56–57, Jan 1959.
- [65] Richard J. Plano. Momentum and asymmetry spectrum of μ -meson decay. *Phys. Rev.*, 119(4):1400–1408, Aug 1960.
- [66] Akhmanov *et al.* *Sov. J. Nucl. Phys*, 6:230, 1968.
- [67] I. Beltrami *et al.* Muon decay: Measurement of the integral asymmetry parameter. *Phys. Lett. B*, 194(2):326–330, 1987.
- [68] Ali-Zade *et al.* *Soviet Phys.-JETP*, 36 (9):940, 1959.

-
- [69] R.S. Hayano *et al.* Search for Right-Handed Currents in the Decay $K^+ \rightarrow \mu^+\nu$. *Phys. Rev. Lett.*, 52(5):329–332, Jan 1984.
- [70] J. Imazato *et al.* Search for right-handed currents in the decay chain $K^+ \rightarrow \mu^+\nu$, $\mu^+ \rightarrow e + \nu\bar{\nu}$. *Phys. Rev. Lett.*, 69(6):877–880, Aug 1992.
- [71] T. Yamanaka *et al.* Search for right-handed currents in the decay $K^+ \rightarrow \mu^+\nu$. *Phys. Rev. D*, 34(1):85–96, Jul 1986.
- [72] C.A. Coombes *et al.* Polarization of μ^+ Mesons from the Decay of K^+ Mesons. *Phys. Rev.*, 108(5):1348–1351, Dec 1957.
- [73] D. Cutts, T. Elioff, and R. Stiening. Muon Polarization and Energy Spectrum in $K^+ \rightarrow \pi^0 + \mu^+ + \nu$. *Phys. Rev.*, 138(4B):B969–B979, May 1965.
- [74] D. Cutts, R. Stiening, C. Wiegand, and M. Deutsch. Measurement of the Muon Polarization Vector in $K^+ \rightarrow \pi^0 + \mu^+ + \nu$. *Phys. Rev.*, 184(5):1380–1392, Aug 1969.
- [75] R.S. Henderson *et al.* Precision planar drift chambers and cradle for the TWIST muon decay spectrometer. *Nucl. Instrum. Methods Phys. Res., Sect. A*, 548:306–335, August 2005.
- [76] J. Hu *et al.* Time expansion chamber system for characterization of TWIST low-energy muon beams. *Nucl. Instrum. Methods Phys. Res., Sect. A*, 566:563–574, October 2006.
- [77] C.J. Oram, J.B. Warren and G.M. Marshall. Commissioning of a new low energy $\pi - \mu$ channel at TRIUMF. *Nucl. Instrum. Methods*, 179:95–103, January 1981.
- [78] J. Doornbos. The tuning of M13 for TWIST, theory and some results. Internal TWIST bulletin boards, December 2000.
- [79] A. Hillairet. *Measurement of δ (in preparation)*. PhD thesis, University of Victoria, 2010.
- [80] R.E. Mischke, TRIUMF, Vancouver, Canada. Private communication.
- [81] T. Prokscha *et al.* The new μ E4 beam at PSI: A hybrid-type large acceptance channel for the generation of a high intensity surface-muon beam. *Nucl. Instrum. Methods Phys. Res., Sect. A*, 595.

-
- [82] J.E. Draper. Beam Steering with Quadrupole and with Rectangular Box Magnets. *Rev. Sci. Instrum.*, 37:1390, October 1966.
- [83] R.P. MacDonald. *A Precision Measurement of the Muon Decay Parameters ρ and δ* . PhD thesis, University of Alberta, 2008.
- [84] J. Musser. *Measurement of the Michel parameter ρ in muon decay*. PhD thesis, Texas A&M University, 2005.
- [85] Vector Fields. OPERA 3D simulation software. <http://vectorfields.com>.
- [86] A. Gaponenko. *A Precision Measurement of the Muon Decay Parameter δ* . PhD thesis, University of Alberta, 2005.
- [87] D. Wright. TN1: DME / He WC Gas Comparison. Technical report, TWIST collaboration, TRIUMF, October 1996.
- [88] R. Openshaw, TRIUMF, Vancouver, Canada. Private communication.
- [89] LeCroy Corporation. 1877 Multihit Time-to-Digital Converter: Specification. <http://www.lecroy.com/lrs/dsheets/1877.htm>.
- [90] LeCroy Corporation. LeCroy 1877 Fastbus TDC Manual.
- [91] R. Brun and F. Rademakers. ROOT - An Object Oriented Data Analysis Framework. *Nucl. Inst. & Meth. in Phys. Res. A*, 389:81–86, 1997.
- [92] CERN Application Software Group. GEANT Detector Description and Simulation Tool, Version 3.21, 1994.
- [93] F. James. Fitting tracks in wire chambers using the Chebyshev norm instead of least squares. *Nucl. Instrum. Methods Phys. Res.*, 211(1):145 – 152, 1983.
- [94] R. Veenhof. Garfield - simulation of gaseous detectors. CERN Program Library W5050.
- [95] P. Depommier. TN49: Muon polarisation in electromagnetic fields. Technical report, TWIST collaboration, TRIUMF, 2001.
- [96] P. Gumplinger, TRIUMF, Vancouver, Canada. Private communication.

- [97] R. Bayes. *Measurement of ρ (in preparation)*. PhD thesis, University of Victoria, 2010.
- [98] G.M. Marshall, TRIUMF, Vancouver, Canada. Private communication.
- [99] R. Armenta. TN68: TWIST Magnet: Field Map Study. Technical report, TWIST collaboration, TRIUMF, 2002.
- [100] M. Simard. Study of the Magnetic Field Map for TWIST at TRIUMF. Technical report, TWIST collaboration, TRIUMF, 2003.
- [101] C. Boucher-Veronneau. The TWIST Solenoid Magnetic Field. Technical report, TWIST collaboration, TRIUMF, 2004.
- [102] S. Fotooshi. Modeling the TWIST Magnet. Technical report, TWIST collaboration, TRIUMF, 2005.
- [103] A. Grossheim, TRIUMF, Vancouver, Canada. Private communication.
- [104] G. Marshall. OPERA map corrections from Hall and NMR maps at 2.0 T. Internal TWIST report, April 2009.
- [105] COMSOL. COMSOL Multiphysics. <http://www.comsol.com>.
- [106] V. Selivanov. TN65: GARFIELD Simulation of the TEC. Technical report, TWIST collaboration, TRIUMF, 2002.
- [107] V. Selivanov. TN65.4: One dimension TEC at $B = 2$ T. Technical report, TWIST collaboration, TRIUMF, 2004.
- [108] P. Depommier. TN96: Muon polarization in the $\pi^+ \rightarrow \mu^+ \nu \gamma$ decay. Technical report, TWIST collaboration, TRIUMF, 2005.
- [109] A. Grossheim *et al.* Decay of negative muons bound in ^{27}Al . *Phys. Rev. D*, 80(5):052012, Sep 2009.
- [110] H. Yukawa. On the Interaction of Elementary Particles. *I, Proc. Phys.-Math. Soc. Jpn.*, 17:48, 1935.
- [111] C.D. Anderson and S.H. Neddermeyer. Cloud Chamber Observations of Cosmic Rays at 4300 Meters Elevation and Near Sea-Level. *Phys. Rev.*, 50:263–271, 1936.

-
- [112] S.H. Neddermeyer and C.D. Anderson. Cosmic-Ray Particles of Intermediate Mass. *Phys. Rev.*, 54:88–89, 1938.
- [113] S.H. Neddermeyer and C.D. Anderson. Nature of Cosmic-Ray Particles. *Rev. Mod. Phys.*, 11:191–207, 1939.
- [114] M. Riordan. *The Hunting of the Quark*. Sage Publications, 1987.
- [115] M. Conversi, E. Pancini and O. Piccioni. On the Disintegration of Negative Mesons. *Phys. Rev.*, 71:209–210, 1947.
- [116] E. Fermi, E. Teller and V. Weisskopf. The Decay of Negative Mesotrons in Matter. *Phys. Rev.*, 71:314–315, 1947.
- [117] C.M.G. Lattes, G.P.S. Occhialini and C.F. Powell. Observations on the Tracks of Slow Mesons in Photographic Emulsions Part 1. *Nature*, 160:453–456, 1947.
- [118] C.M.G. Lattes, G.P.S. Occhialini and C.F. Powell. Observations on the Tracks of Slow Mesons in Photographic Emulsions Part 2. *Nature*, 160:486–492, 1947.
- [119] T.D. Lee. A Brief History of the Muon. *Hyperfine Interact.*, 86:439–453, 1994.
- [120] C.S. Wu and V.W. Hughes. *Muon Physics: Introduction and History*. Academic Press Inc., 1977.
- [121] R.A. Millikan. Mesotron as the Name of the New Particle. *Phys. Rev.*, 1:105, December 1938.
- [122] C.D. Anderson and S.H. Neddermeyer. Mesotron (Intermediate Particle) as a Name for the New Particles of Intermediate Mass. *Nature*, 142:878, November 1938.
- [123] H. Lyle. Anderson, Carl. Interview by Harriett Lyle. Oral History Project, California Institute of Technology. Retrieved April 2008 from the World Wide Web: http://resolver.caltech.edu/CaltechOH:OH_Anderson_C, 1979.
- [124] A.H. Compton. Foreword: Symposium on Cosmic Rays. *Rev. Mod. Phys.*, 11:122, 1939.
- [125] H.J. Bhabha. The Fundamental Length Introduced by the Theory of the Mesotron (Meson). *Nature*, 143:276–277, February 1939.

- [126] J. L. Beveridge *et al.* A spin rotator for surface μ^+ beams on the new M20 muon channel at TRIUMF. *Nucl. Instrum. Methods Phys. Res., Sect. A*, 240:316–322, 1985.
- [127] Triumf CMMS. Helios superconducting solenoid. Website: <http://cmms.triumf.ca/equip/helios.html>.
- [128] G. Morris, TRIUMF, Vancouver, Canada. Private communication.
- [129] S.R. Dunsiger *et al.* Magnetic field dependence of muon spin relaxation in geometrically frustrated $\text{Gd}_2\text{Ti}_2\text{O}_7$. *Phys. Rev. B*, 73(172418), 2006.
- [130] F. James. MINUIT – Function Minimization and Error Analysis, CERN Program Library Entry D 506.
- [131] J.F. Ziegler. The stopping and range of ions in matter. <http://www.srim.org/>.
- [132] TRIUMF CS. TRIUMF Computing Services description of SRIM. <http://it-services.triumf.ca/scientific-computing/software/detector-engineering/srim-1>.
- [133] D.M. Garner. *Application of the muonium spin rotation technique to a study of the gas phase chemical kinetic of muonium reactions with the halogens and hydrogen halides*. PhD thesis, University of British Columbia, June 1979.
- [134] J. Doornbos, TRIUMF, Vancouver, Canada. Private communication.